10. E. Dlan, J. Miller, and W. Schilders, Numerical Difference Methods of Solving Boundary-Layer Problems [Russian translation], Moscow (1983).
11. C. de Boer, A Practical Handbook on Splines [Russian translation], Moscow (1985).
12. S. Minkov and A. Minchev, Zh. Prikl. Khim., 59, No. 12, 2704 (1986).
13. P. G. Romankov, N. B. Rashkovskaya, and V. F. Frolov, Mass Transfer in Chemical Engineering [in Russian], Leningrad (1985).

EMISSIVITY MEASUREMENT FOR A CARBON–CARBON COMPOSITE AND A PHENOLIC CARBON PLASTIC

L. S. Slobodkin and M. Ya. Flyaks

UDC 535.231:535.343.2

Two equipments have been used together to determine composite-material emissivity at high temperatures; measurements are reported on the normal emissivities of carbon-based composites.

Carbon–carbon composites and phenolic carbon-filled plastics can be used to make items operating over wide heat-flux ranges, including very high ones [1]. Usually, radiative heat exchange is important, and often decisive, so emissivity data are essential to determine heat transfer and to design components to be subject to intense heat loads. The methods and apparatus for the corresponding measurements are also very important.

The published data on the emissivities of phenolic plastics and carbon–carbon composites are extremely limited and fragmentary [2]. In [3], measurements were reported for $\varepsilon_{\lambda n}$ for a phenol-graphite composite at 2500 K at 0.3-10 μm, while in [4] there are data on the spectral emissivities of coked residues from phenolic carbon at 2550 and 2850 K for 0.4-2.8 μm. There are also data [5, 6] on the emissivities of heat-protective materials based on a carbon–carbon composite with various additives.

Here we describe an apparatus for determining composite emissivities and give measurements on carbon–carbon composites at 700-2000 K.

Two equipments are used in measuring the emissivity at 700-2000 K: one of them is the LIST-5A (Fig. 1a), which is used in determining the temperature dependence of the monochromatic normal-hemispherical reflectivity $\rho_{\lambda n,2\pi}(T)$ in the near IR at 1.0 μm at 700-1400 K and in the visible region at λ = 0.58 μm at 1100-2000 K. The specimen 1 is placed at the center of the integrating sphere 2, which also contains the radiation sources: KI-220-1000 halogen filament lamps and DRT-1000-4 mercury in quartz lamps. The specimen is heated by the beams from the carbon dioxide lasers 6 and 7 working at 10.6 μm. The beam intensities are controlled by the attenuators 9. The recording system consists of the measuring instrument 10 based on an EOP-66 standard optical pyrometer, which is used in the visible region, and the VIMP-015M micropyrometer 5, which makes measurements at 1.0 μm.

One determines $\rho_{\lambda n,2\pi}$ in the visible and near-IR ranges by comparing the radiation fluxex reflected by the specimen and standard; the latter is composed of magnesium oxide deposited on a cassette placed by the specimen at the center. The basic component here is the means of isolating the reflected radiation from the total flux (inherent and reflected). When one determines $\rho_{\lambda n,2\pi}$ at 1.0 μm, the VIMP-015M measures the brightness temperatures of the specimen with the KI-220-1000 lamps on and off and for the standard with the sources on. In order to use the standard pyrometer calibration, the radiation from the object is attenuated if necessary by a filter having transmission τ. The formula is

$$\rho_{\lambda n,2\pi}=\left\{\frac{\tau_{st}}{\tau_s}\exp\frac{C_2}{\lambda}\left(\frac{1}{T'_{st}}-\frac{1}{T'_s}\right)-\frac{\tau_{st}}{\tau_0}\exp\frac{C_2}{\lambda}\left(\frac{1}{T'_{st}}-\frac{1}{T'_i}\right)\right\}\rho^{st}_{\lambda n,2\pi}, \quad (1)$$

Lykov Institute of Heat and Mass Transfer, Belorussian Academy of Sciences, Minsk.
Translated from Inzhenerno-Fizicheskii Zhurnal, Vol. 57, No. 2, pp. 308-313, August, 1989. Original article submitted March 4, 1988.

 0022-0841/89/5702-0972$12.50

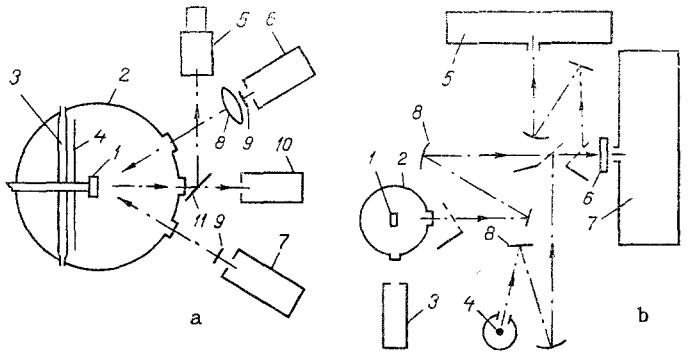

Fig. 1. Apparatus for determining $\rho_{\lambda n, 2\pi}$ (a) and $\varepsilon_{\lambda\alpha}$ (b): a – 1) specimen; 2) integrating sphere; 3) sources; 4) reflector; 5) VIMP-015M micropyrometer; 6) LGN-701 laser; 7) LG-22 laser; 8) lens; 9) attenuators; 10) measurement instrument; 11) mirror; b – 1) specimen; 2) chamber; 3) pyrometer; 4) intermediate standard; 5) monochromator and detector for the visible region; 6) modulator; 7) monochromator and detector for the infrared region; 8) mirrors.

in which T' is the brightness temperature of the object as observed through the filter having transmission τ. See [7] for the derivation of (1) and a detailed description of the apparatus and method.

When $\rho_{\lambda n, 2\pi}$ is measured in the visible region, the line-spectrum mercury-quartz lamps are used as sources. The total brightness due to the inherent radiation and reflected beam is recorded in a band λ_i corresponding to one of the peaks in the source spectrum, while the inherent radiation is recorded at a wavelength λ_j near λ_i. In particular, to measure $\rho_{\lambda n, 2\pi}$ for these composites, we used $\lambda_i = 0.58$ μm and $\lambda_j = 0.60$ μm.

The formula is

$$\rho_{\lambda n, 2\pi} = \frac{R_s(\lambda_i) - R_i(\lambda_j)}{1 - R_{st}(\lambda_i, \lambda_j)} \rho^{st}_{\lambda n, 2\pi}, \qquad (2)$$

in which $R_s(\lambda_i) = I_{\lambda n}{}^s(\lambda_i)/I_{\lambda n}{}^{st}(\lambda_i)$; $R_i(\lambda_j) = I_{\lambda n}{}^i(\lambda_j)/I_{\lambda n}{}^{st}(\lambda_i)$; $R_{st}(\lambda_i, \lambda_j) = I_{\lambda n}{}^{st}(\lambda_j)/I_{\lambda n}{}^{st}(\lambda_i)$. It is assumed that as λ_i and λ_j are close together, $\varepsilon_{\lambda n}(\lambda_i) = \varepsilon_{\lambda n}(\lambda_j)$, and as the source spectrum consists of lines, the reflected radiation at 0.60 μm is weak, so $R_{st}(\lambda_i, \lambda_j)$, which characterizes the brightness ratio for the standard at 0.60 and 0.58 μm, did not exceed 0.03. The method of measuring $\rho_{\lambda n, 2\pi}$ in the visible region is analogous to that used with the LIST-3, for which a detailed description has been given in [8] along with the derivation of (2). The reflectivity of the standard $\rho_{\lambda n, 2\pi}{}^{st}$ is measured in advance by comparing the brightnesses from the standard coating and the surface of the integrating sphere. To improve the accuracy in measuring $\rho_{\lambda n, 2\pi}{}^{st}$, the radiation sources and specimen holder are removed from the sphere. All the windows and holes are closed, apart from the two intended correspondingly for sighting on the object and introducing the radiation from an external source. The source was the illuminating device from VSU2-P spectrometer.

The second equipment (Fig. 1b) is used to measure $\varepsilon_{\lambda\alpha}(\lambda)$ for the composites at 700-2000 K. The specimen 1 in the water-cooled chamber 2 is heated by a graphite or tantalum heater bearing a current. A wide measurement range is provided by two monochromators: 5 for the visible and 7 for the infrared, which work with three detectors: a bolometer and two photoelectric detectors for the ranges 0.20-0.60 and 0.60-1.1 μm. The mirror system 8 images the object on the onochromator slits. One determines $\varepsilon_{\lambda n}$ by comparing the radiation from the specimen with that from a black body model at the same temperature:

$$\varepsilon_{\lambda n} = \frac{I^i_{\lambda n}}{I^{bb}_{\lambda n}} \varepsilon^{bb}_{\lambda n}. \qquad (3)$$

The black body is used in place of the specimen and the radiation fluxes are recorded at various wavelengths at set temperatures. Then the same entrance slit is used in measuring

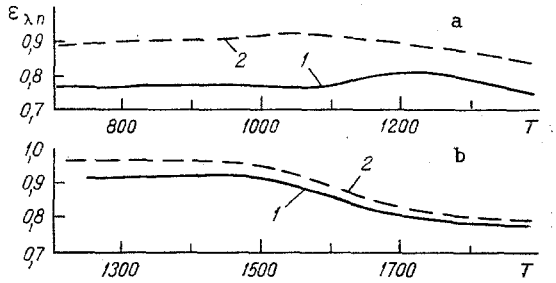

Fig. 2. Temperature dependence of $\varepsilon_{\lambda n} = 1 - \rho_{\lambda n, 2\pi}$. a) λ = 1.0 μm; b) 0.58. 1) carbon–carbon composite; 2) phenolic carbon plastic.

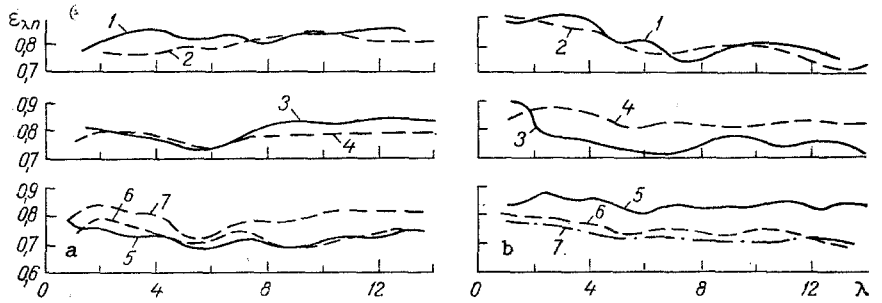

Fig. 3. Spectral normal emissivity for carbon–carbon composite (a) and phenolic carbon plastic (b): 1) T = 730 K; 2) 980; 3) 1240; 4) 1420; 5) 1540; 6) 1700; 7) 1990 K. λ, μm.

the fluxes from the specimen at the black-body temperature. The black body is a graphite tube having a rectangular slot in the side and heated by a current. The power supply provides up to 35 kW with smooth adjustment over the range 300-1700 A. The main difficulty in measuring $\varepsilon_{\lambda\alpha}$ is associated with determining the true surface temperature, which is very important for these composites, which often have low thermal conductivities and thus considerable temperature gradients. The difficulties are overcome by the use of the $\rho_{\lambda n, 2\pi}$ data obtained with the LIST-5A, which enable one to determine the true temperature and then measure $\varepsilon_{\lambda\alpha}$ in the appropriate spectral rnge. The two equipments supplement one another and form a suite giving a combined method of determining $\varepsilon_{\lambda\alpha}$.

This suite was used to determine emissivities for two materials: a carbon–carbon composite and a phenolic carbon plastic, which were used at 1.3-13 Pa (10^{-1}-10^{-2} mm Hg). Here the relative error in determining $\varepsilon_{\lambda n}$ at 1-14 μm and $\varepsilon_{\lambda n} = 1 - \rho_{\lambda n, 2\pi}$ at 0.58 and 1.0 μm did not exceed 4% for the 0.95 confidence range.

Figure 2 shows that the temperature dependence of $\varepsilon_{\lambda n}$ at 1.0 μm is slight for both. Above 1500 K, $\varepsilon_{\lambda n}$ has a negative temperature coefficient at 0.58 μm. In both cases, the blackness of the phenolic plastic was higher than that of the carbon–carbon composite, the difference being greater for $\varepsilon_{\lambda n}$ at 1 μm. The spectral normal emissivity for the carbon–carbon composite was 0.69-0.86 in these ranges in T and λ (Fig. 3a). The wavelength dependence of $\varepsilon_{\lambda n}$ alters with temperature, since it changes from 0.78 to 0.86 at 730 K, i.e., by 10%, while at 1990 K it goes from 0.69 to 0.84, i.e., 22% change. The values for the phenolic material (Fig. 3b) in these T and λ ranges are 0.71-0.91. At 730 K, $\varepsilon_{\lambda n}$ ranges from 0.75 to 0.91 (21% change), while at 1540 K, the change was from 0.81 to 0.88, i.e., 9%. In neither case did the $\varepsilon_{\lambda n}(\lambda)$ curve show any prominent peaks, minima, or other singularities.

The $\varepsilon_{\lambda n}$ ranges here did not differ greatly from those in [6] for a carbon–carbon composite containing additives, where $\varepsilon_{\lambda n}$ was 0.70-0.96. On the other hand, the spectral normal blackness at 0.6-4 μm for the [5] material was much lower than for our composites, perhaps because the [5] specimen contained silicon dioxide, which has low blackness in the visible and near-IR ranges.

We calculated the partial integral normal degrees of blackness $\varepsilon_{\Sigma n}$ from the $\varepsilon_{\lambda n}$ at 1-14 μm and those for 0.58 μm. In the range 0.58-14 μm, one finds from 92% of the integral radia-

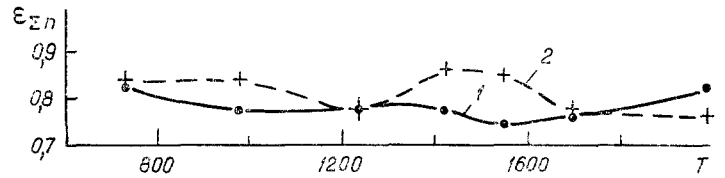

Fig. 4. Integral normal emissivities: 1) carbon–carbon composite; 2) phenolic carbon plastic.

tion flux for a black body (at 730 K) to 98% (at 2000 K), so the partial and total integral normal emissivities are similar. Figure 4 shows that $\varepsilon_{\Sigma n}$ varies slightly with temperature but is always in the range 0.75-0.85. The values are similar as regards level and temperature dependence to the $\varepsilon_{\Sigma n}$ for a heat-protection material based on a carbon–carbon composite as given in [5] for 800-1400 K and the recommended [9] $\varepsilon_{\Sigma n}$ for artificial graphites at 1200-2000 K.

NOTATION

$\rho_{\lambda n, 2\pi}$, monochromatic normal hemispherical reflectivity; $\varepsilon_{\lambda\alpha}$, $\varepsilon_{\lambda n}$, spectral directional and normal emissivities; λ, wavelength; T, temperature in K; T', brightness temperature of object observed through filter; τ, filter transmission used in sighting object; $C_2 = 1.438 \cdot 10^{-2}$ m×K; $I_{\lambda n}$, spectral normal brightness. Subscripts: n, normal; i, inherent emission; s, summary inherent and reflected radiation; st, standard; bb, black body.

LITERATURE CITED

1. S. Park, J. H. Landell, M. J. Green, V. Vanovich, and M. A. Covington, Aerospace Engineering [Russian translation], 3, No. 5, 50-61 (1985).
2. N. A. Rubtsov and E. I. Averkov, Prom. Teplotekh., 5, No. 5, 75-87 (1983).
3. Chang and Sutton, Rocket Engineering and Space Sciences [Russian translation], 7, No. 6, 147-153 (1969).
4. Wilson and Spitzer, Rocket Engineering and Space Sciences [Russian translation], 7, No. 11, 117-119 (1969).
5. L. M. Grinberg, R. G. Luce, and F. K. McGinnis, AIAA Paper No. 144, 1-7 (1976).
6. L. S. Slobodkin, M. Ya. Flyaks, and B. V. Andreev, Theory and Practice in Moist-Material Drying [in Russian], Minsk (1979), pp. 16-29.
7. L. S. Slobodkin and M. Ya. Flyaks, Heat and Mass Transfer: Surveys and Prospects [in Russian], Minsk (1985), pp. 115-118.
8. L. S. Slobodkin, M. Ya. Flyaks, and B. V. Andreev, Inzh.-Fiz. Zh., 42, No. 3, 442-448 (1982).
9. A. E. Sheindlin (ed.), Solid-Material Emissivities [in Russian], Moscow (1974).